Supplementary Figures

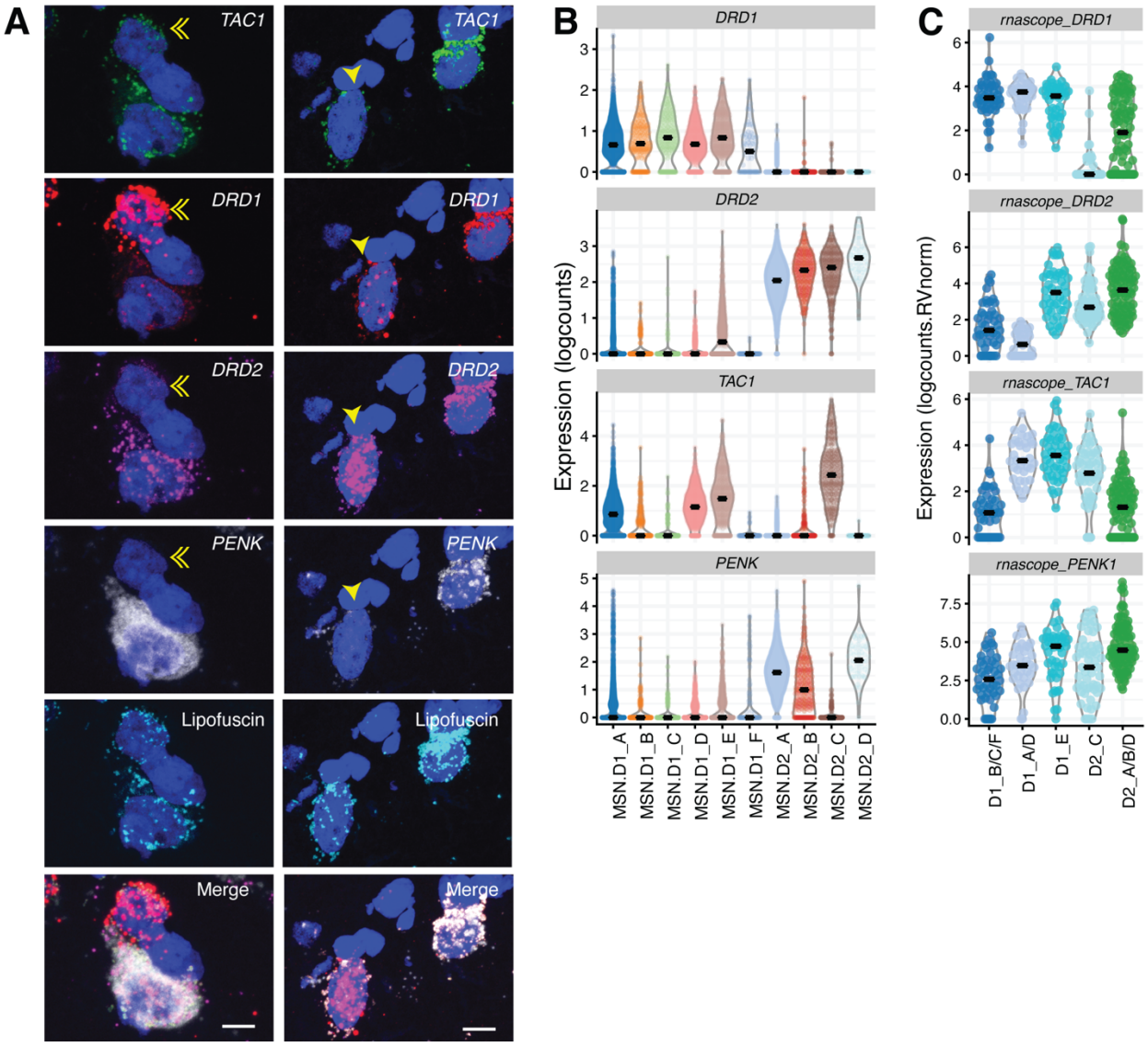

Figure S1. Differential expression of neuropeptide genes *TAC1* and *PENK* in D1 and D2 MSN subpopulations. Multiplex single molecule fluorescent in situ hybridization (smFISH) in human NAc. (**A**) Maximum intensity confocal projections showing expression of DAPI (nuclei), *DRD1*, *DRD2*, *TAC1, and PENK* and lipofuscin autofluorescence in two separate fields. Merged image without lipofuscin autofluorescence. Scale bar=10 µm. Double arrow indicates TAC1 negative D1 MSN. Single arrow indicates dual D1 and D2-expressing MSN. **(B)** Corresponding violin plots showing differential (log_2) expression of *TAC1* and *PENK* in D1 and D2 MSN cell classes. **(C)** Log_2 expression of respective transcript counts per smFISH ROI (ROI size-normalized), post lipofuscin-masking (autofluorescence). Each *DRD1*+ or *DRD2*+ ROI was classified into a Euclidean distance-predicted MSN class (or group of classes) and its (/their) respective expression. Related to **Figure 1** and **Table S5**.

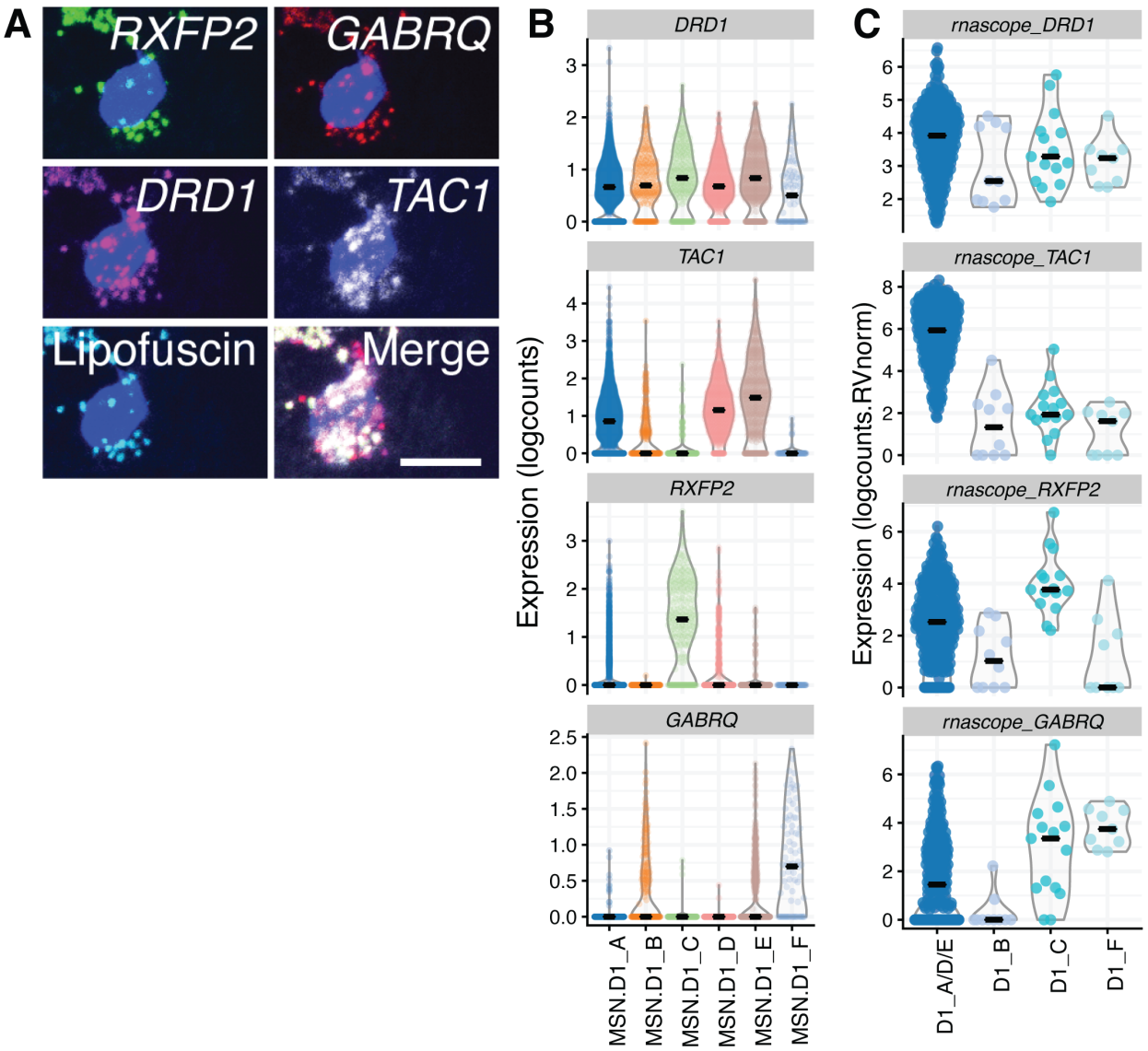

Figure S2. Further validation of D1 MSN subpopulations using smFISH. (A) Multiplex single molecule fluorescent in situ hybridization (smFISH) in human NAc depicting an D1_A, _E, or _E MSN. Maximum intensity confocal projections showing expression of DAPI (nuclei), *RXFP2*, *GABRQ*, *DRD1*, *TAC1* and lipofuscin autofluorescence. Merged image without lipofuscin autofluorescence. Scale bar=10 µm. **(B)** Corresponding violin plots showing differential (log_2) expression of these three genes in specific D1 subpopulations by snRNAseq. **(C)** Log_2 expression of respective transcript counts per smFISH ROI (ROI size-normalized), post lipofuscin-masking (autofluorescence). Each *DRD1*+ ROI was assigned to a Euclidean distance-predicted D1 MSN class (or group of classes) and its (/their) respective expression, showing possible identification of the less abundant D1_C class. Related to **Figure 1** and **Table S5**.

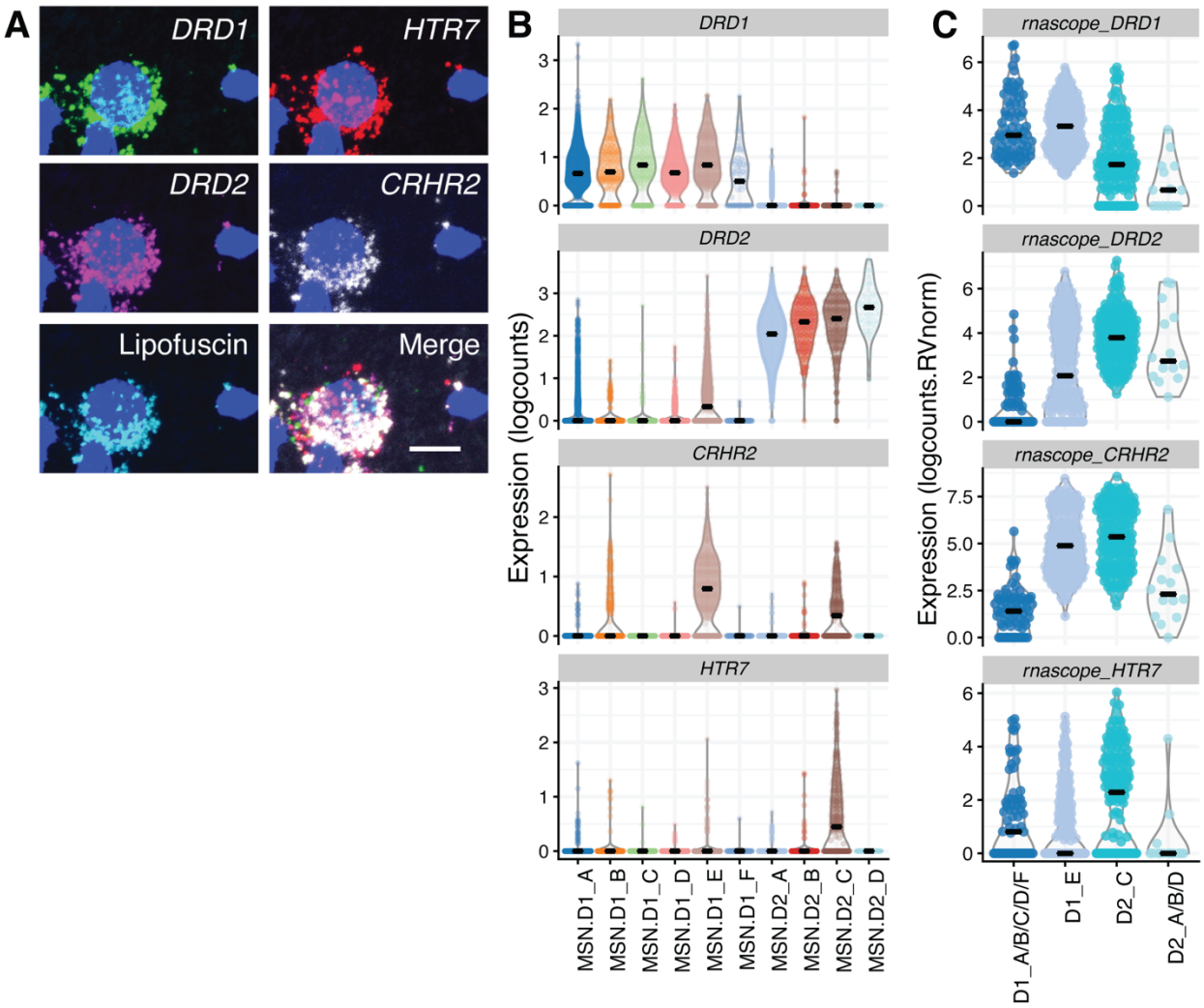

Figure S3. Confirmation of *HTR7*-expressing D2 MSNs in human NAc by smFISH. (A) Multiplex single molecule fluorescent in situ hybridization (smFISH) in human NAc depicting expression of *HTR7* in a D2_C MSN. Maximum intensity confocal projections showing expression of DAPI (nuclei), *DRD1*, *HTR7*, *DRD2*, *CRHR2* and lipofuscin autofluorescence. Merged image without lipofuscin autofluorescence. Scale bar=10 µm. **(B)** Corresponding violin plots showing differential expression of *HTR7* and *CRHR2* in D1 and D2 MSNs subpopulations by snRNA-seq. **(C)** Log_2 expression of respective transcript counts per smFISH ROI (ROI size-normalized), post lipofuscin-masking (autofluorescence). Each *DRD1*+ or *DRD2*+ ROI was assigned to a Euclidean distance-predicted MSN class (or group of classes) and its (/their) respective expression. Related to **Figure 1** and **Table S5.**

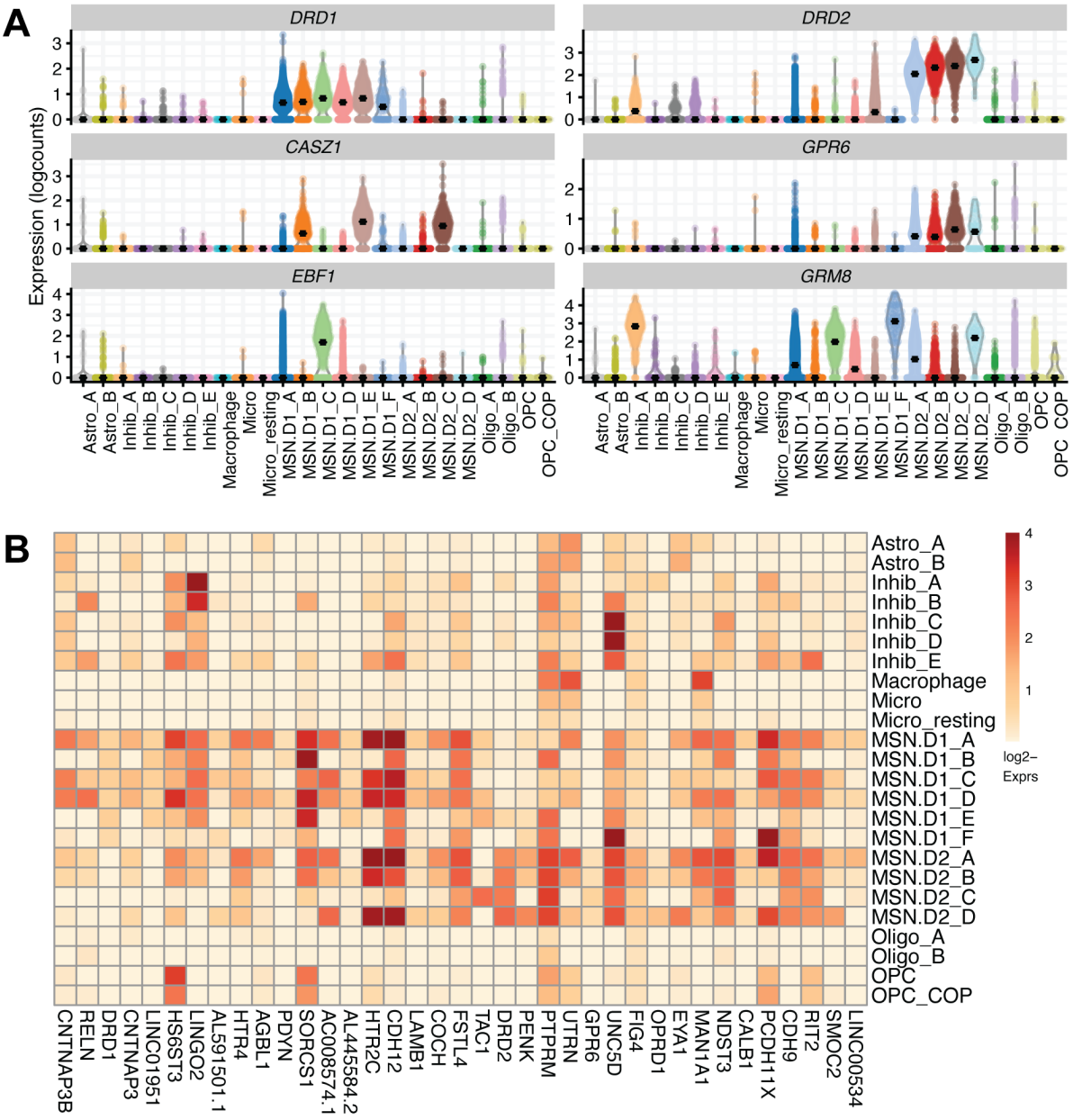

Figure S4. Other differentially expressed MSN markers and similarity between largest D1/D2 subpopulations. (A) Log_2-normalized counts of other markers for MSN subpopulations not prioritized for smFISH validation, as above. *GRM8* is included to show specific enrichment in a variety of D1 or D2 classes. **(B)** Heatmap of mean snRNA-seq expression, showing broad coexpression of the combined top 20 markers for classes D1_A and D2_A (scale thresholded to mean log_2-normalized counts = 4.0). Related to **Figure 1** and **Table S5**.

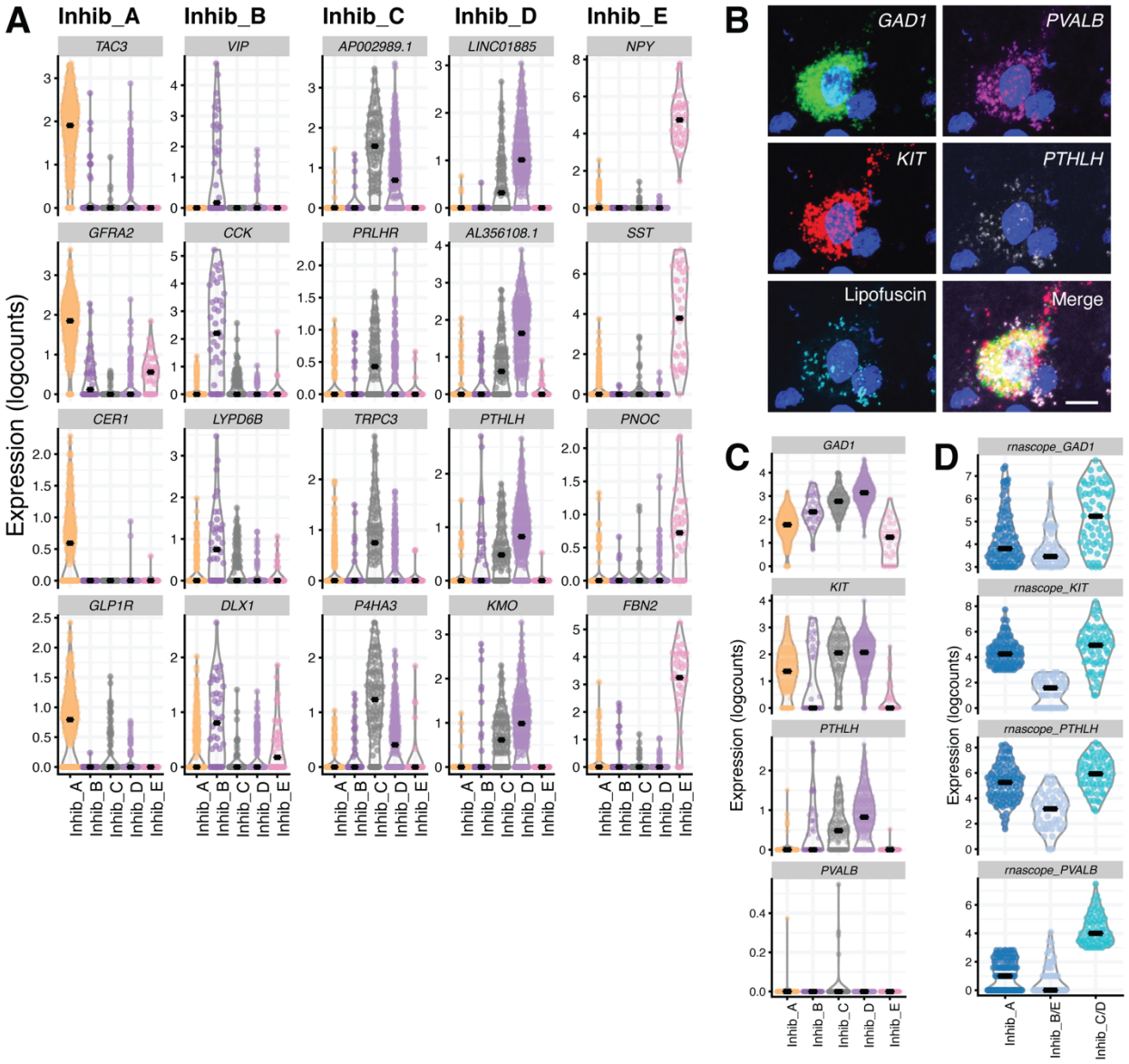

Figure S5. Characterization of interneuron subpopulations in human NAc. (**A)** Violin plots depicting top 4 genes in each GABAergic inhibitory neuron class (columns) in NAc snRNA-seq. **(B)** Multiplex single molecule fluorescent in situ hybridization (smFISH) in human NAc depicting co-expression of *PVALB, KIT,* and *PTHLH* in *GAD1*+ inhibitory neurons. Maximum intensity confocal projections showing expression of DAPI (nuclei), *GAD1*, *PVALB*, *KIT*, *PTHLH* and lipofuscin autofluorescence. Merged image without lipofuscin autofluorescence. Scale bar=10 µm. (**C)** Corresponding violin plots showing (log_2) expression of these genes in different interneuron classes by snRNA-seq. **(D)** Log_2 expression of respective transcript counts per smFISH ROI (ROI size-normalized), post lipofuscin-masking (autofluorescence). Each *GAD1*+ ROI was assigned to a Euclidean distance-predicted interneuron class (or group of classes) and its(/their) respective expression. Related to **Figure 1** and **Table S5**.

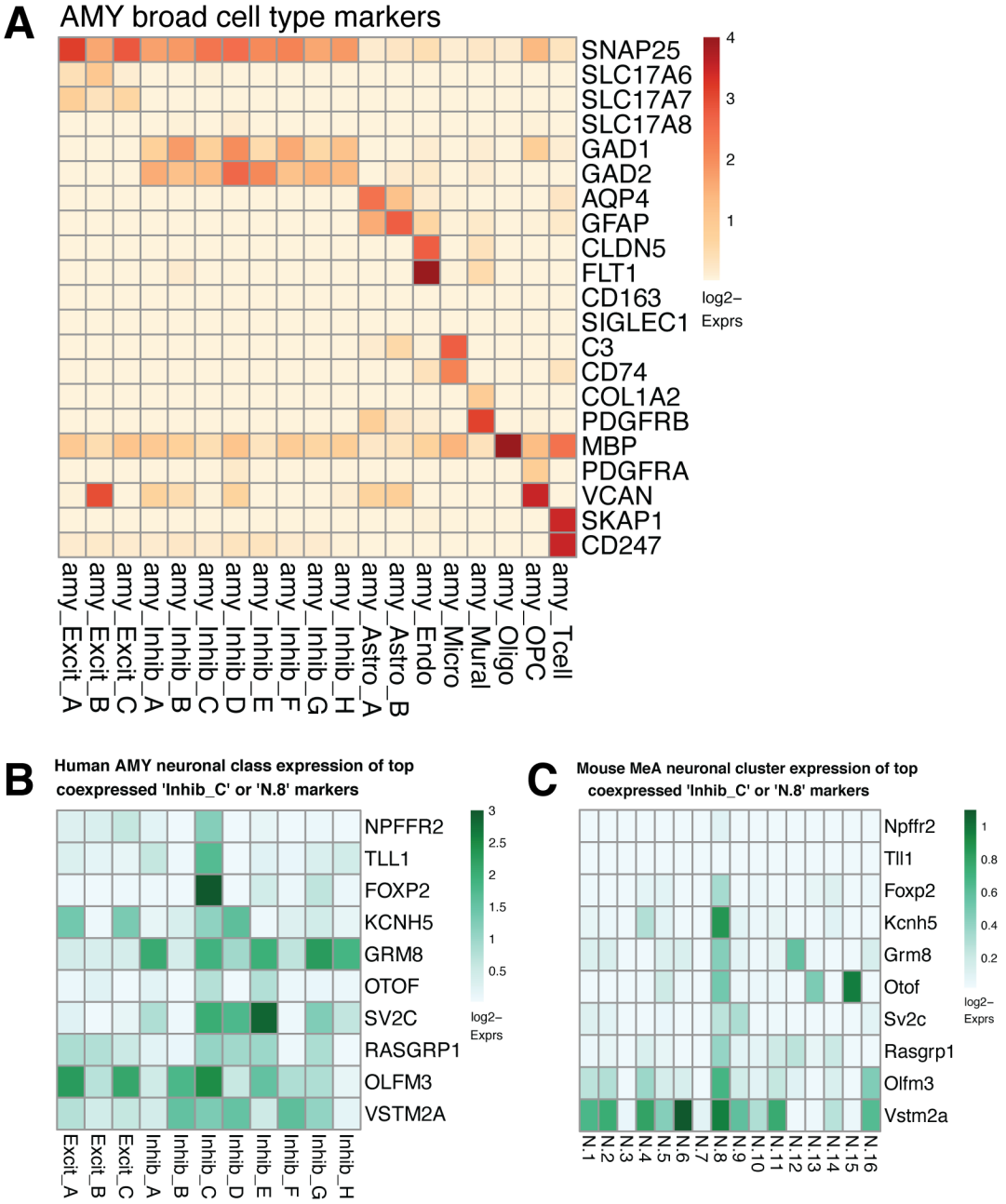

Figure S6. Broad cell type marker expression for AMY subpopulations and 'Inhib.5' vs. corresponding MeA 'N.8' shared markers. (A) Mean $\log_2$-normalized expression for broad cell type markers, used for annotation of AMY cell classes. **(B)** Mean expression of top enriched markers for human AMY subpopulation Inhib_C shared with **(C)** mouse MeA neuronal subclusters, as reported in (Chen et al., 2019). *Tll1*, however, was not defined as a marker of MeA 'N.8'. Related to **Figure 2** and **Table S5**.

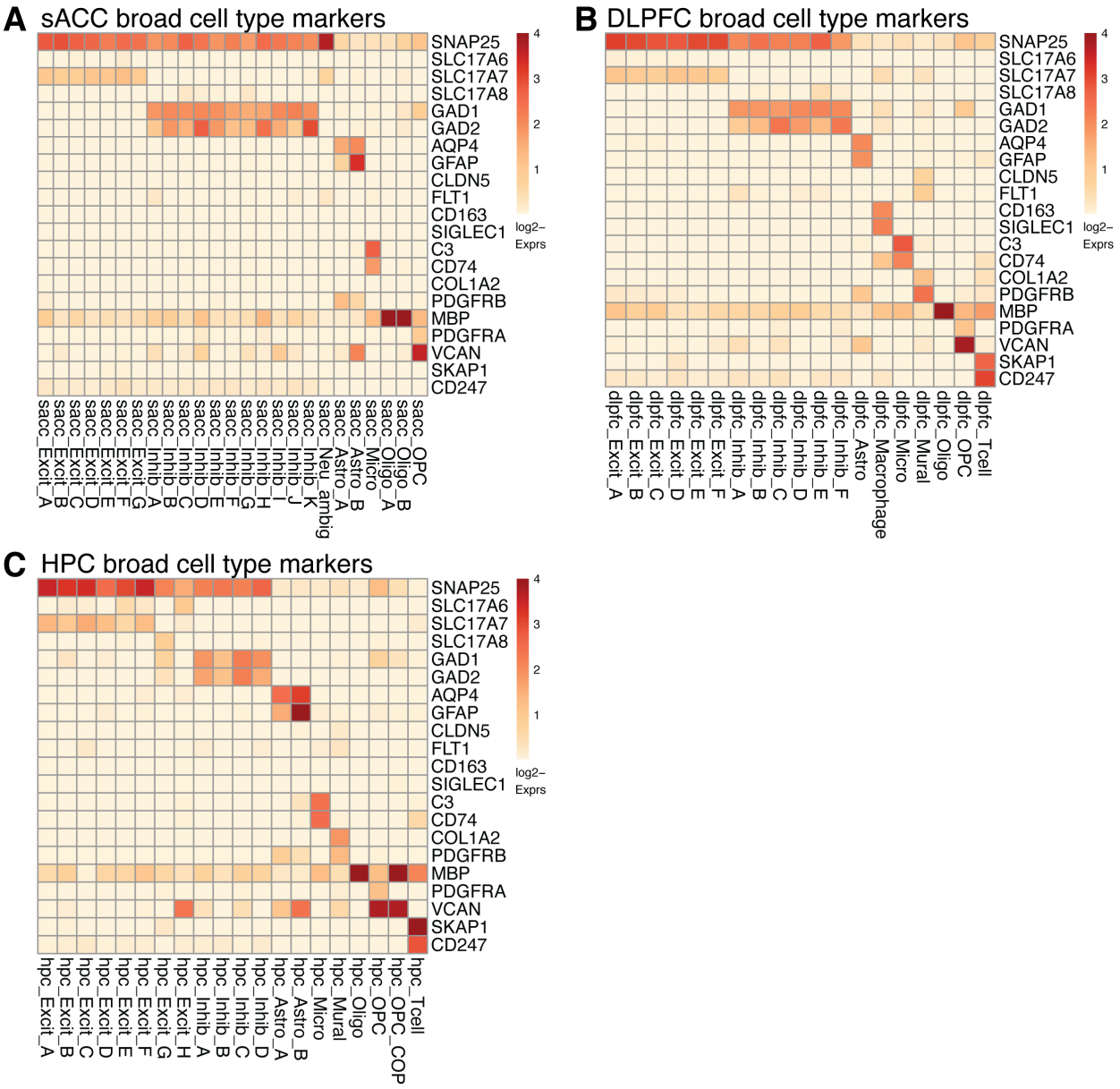

Figure S7. Broad cell type marker expression for pan-brain-defined clusters or regionally-defined populations. (A) Mean $\log_2$-normalized expression for broad cell type markers, used for annotation (or identified, post hoc), in clusters defined within sACC nuclei. **(B)** Same as (A), but for DLPFC, and **(C)** HPC. Related to **Figure 3** and STAR Methods.

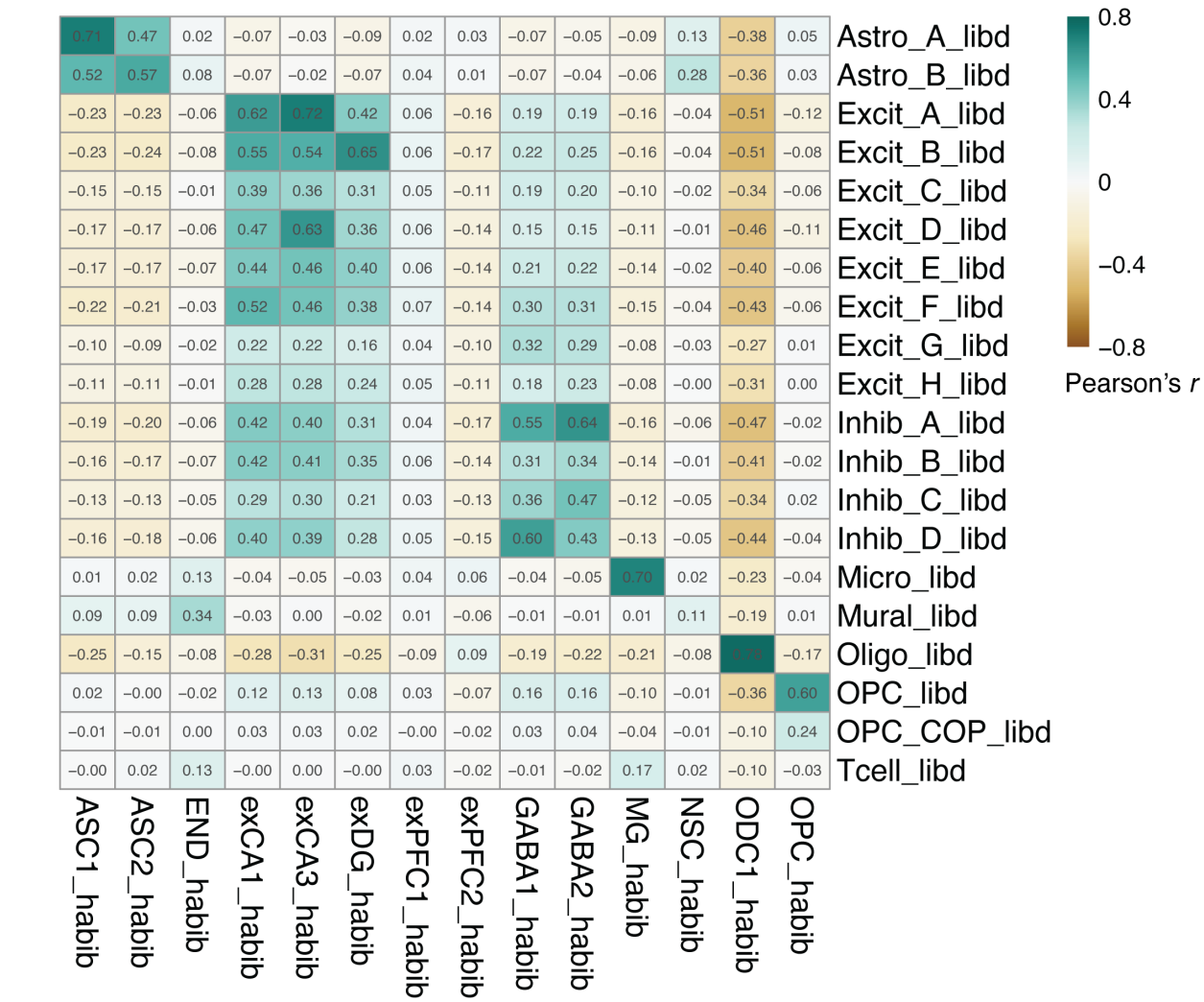

Figure S8. Benchmarking of HPC cell classes to published data. (A) Correlation heatmap between HPC subclusters (rows) and the reported HPC populations in (Habib et al., 2017); columns). Printed values and scales show the Pearson correlation coefficient (*r*), correlating across all shared expressed genes and the *t*-statistics of their specificity test. Related to STAR Methods.

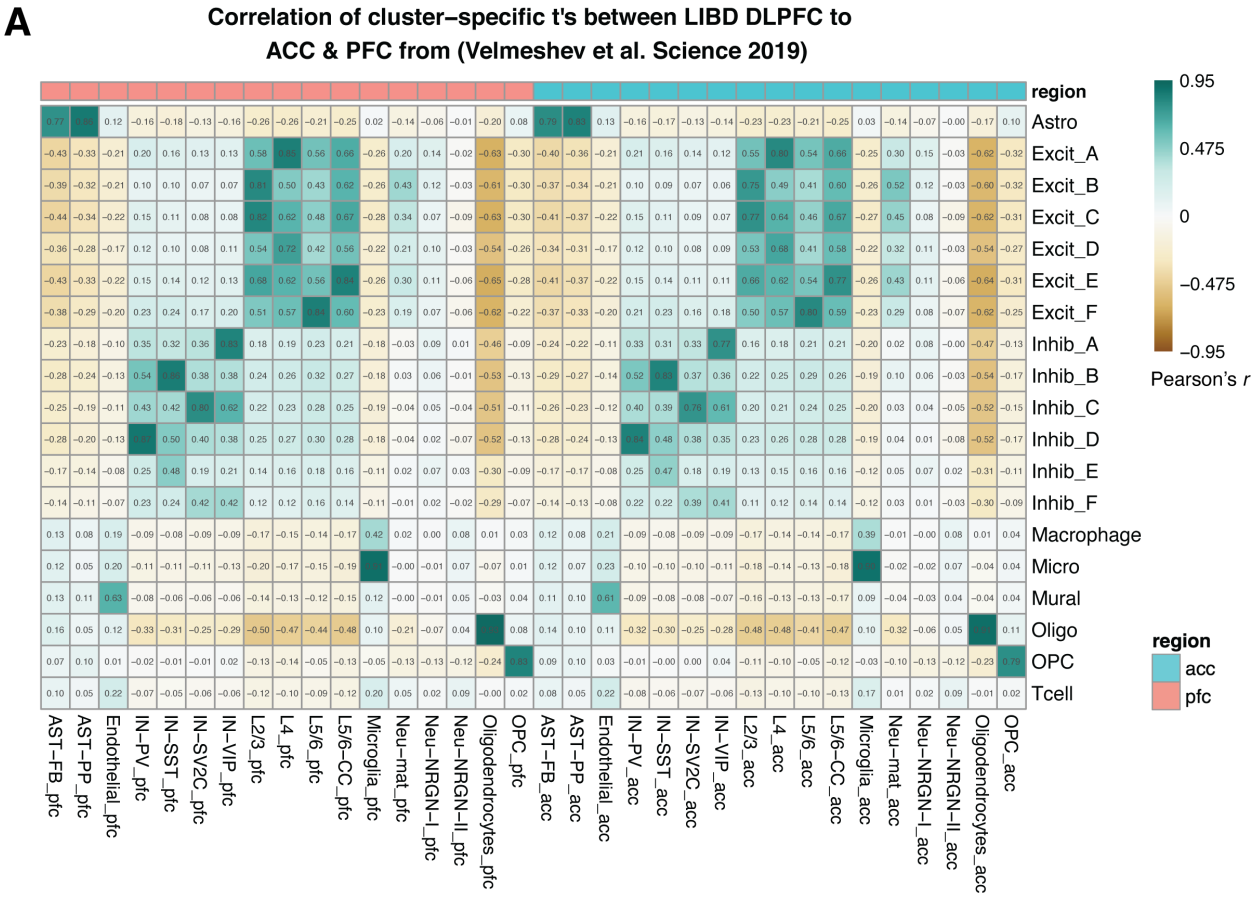

Figure S9. Benchmarking of DLPFC subpopulations to published data. (A) Correlation heatmap between DLPFC spatially-registered subpopulations (rows) and split-PFC and ACC 10x snRNA-seq clusters (columns) from (Velmeshev et al., 2019). Printed values and scales show the Pearson correlation coefficient, correlating across all shared expressed genes (26,970) and the *t*-statistics of their specificity test. Related to STAR Methods.

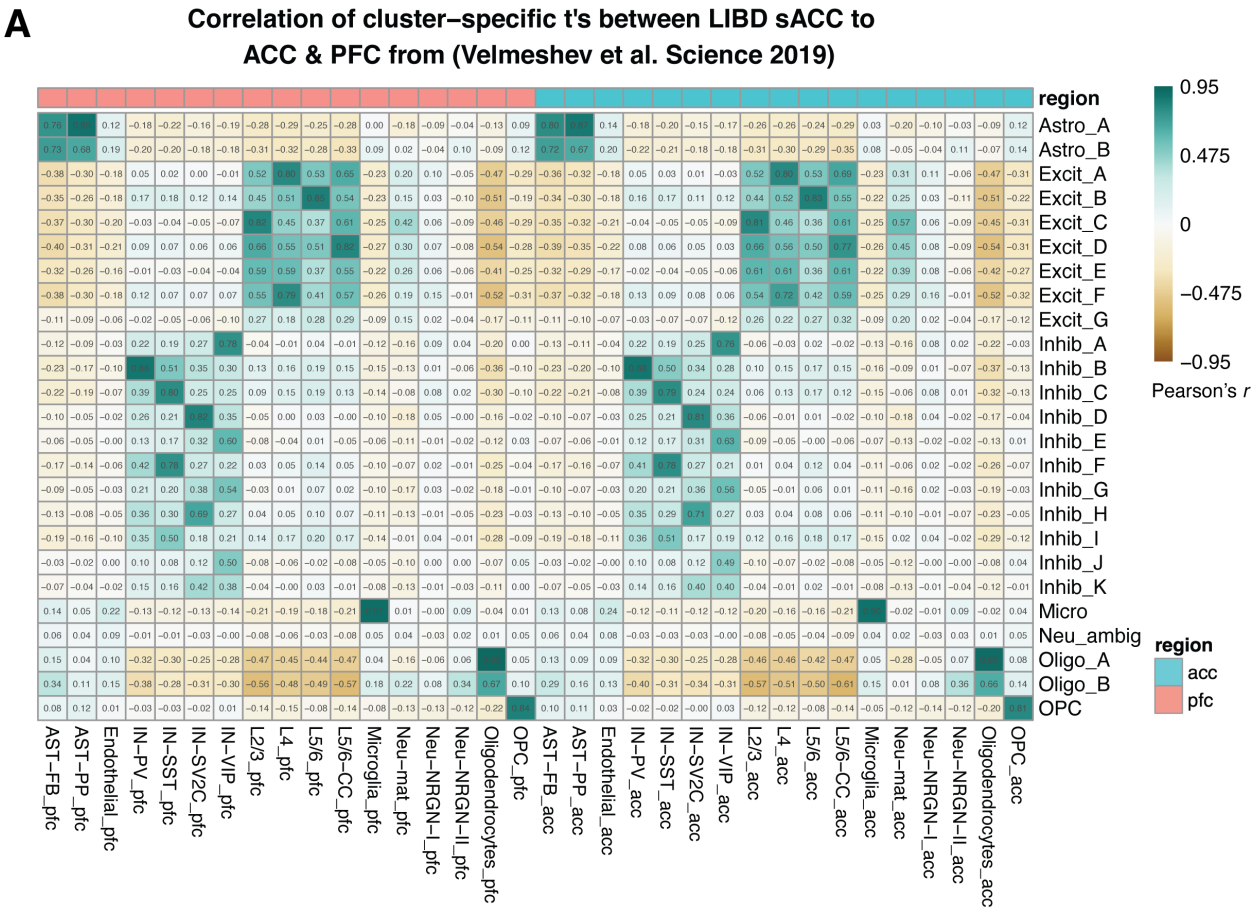

Figure S10. Benchmarking of sACC subpopulations to published data. (A) Correlation heatmap between sACC subpopulations (rows) and split-PFC and ACC 10x snRNA-seq clusters (columns) from (Velmeshev et al., 2019). Printed values and scales show the Pearson correlation coefficient, correlating across all shared expressed genes (27,890) and the *t*-statistics of their specificity test. Related to STAR Methods.

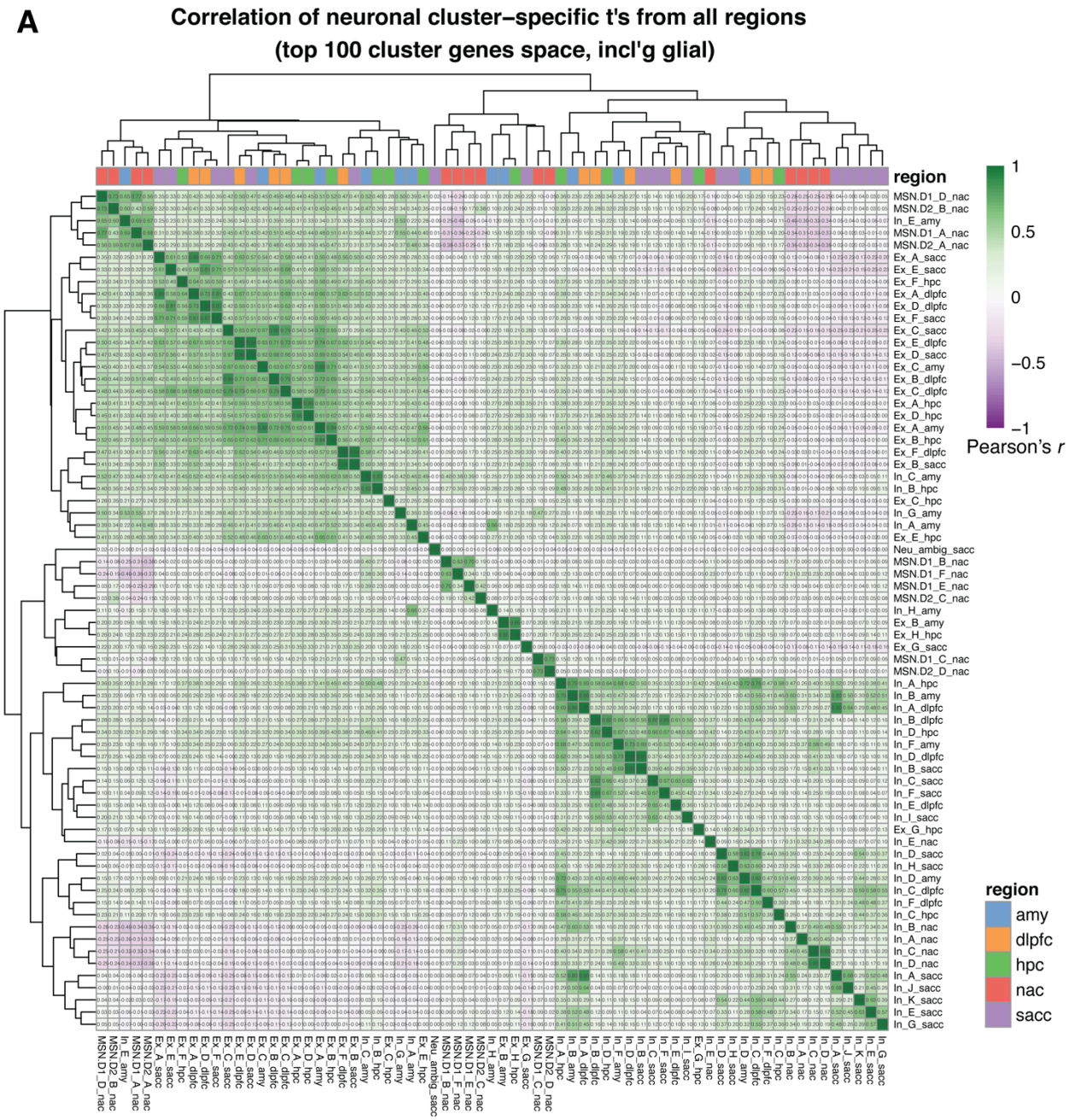

Figure S11. Comparison across all neuronal, regionally-defined subpopulations. Pairwise correlation of *t*-statistics, comparing the top cell class marker genes of the total of 107 classes reported across the five brain regions (total of 3,715 genes). Here, the 69 neuronal classes are shown, as in **Figure 3B**, but with their Pearson correlation coefficient (*r*), printed in each cell. Regions are colored and labeled in the suffix. Scale values are of Pearson's *r*.

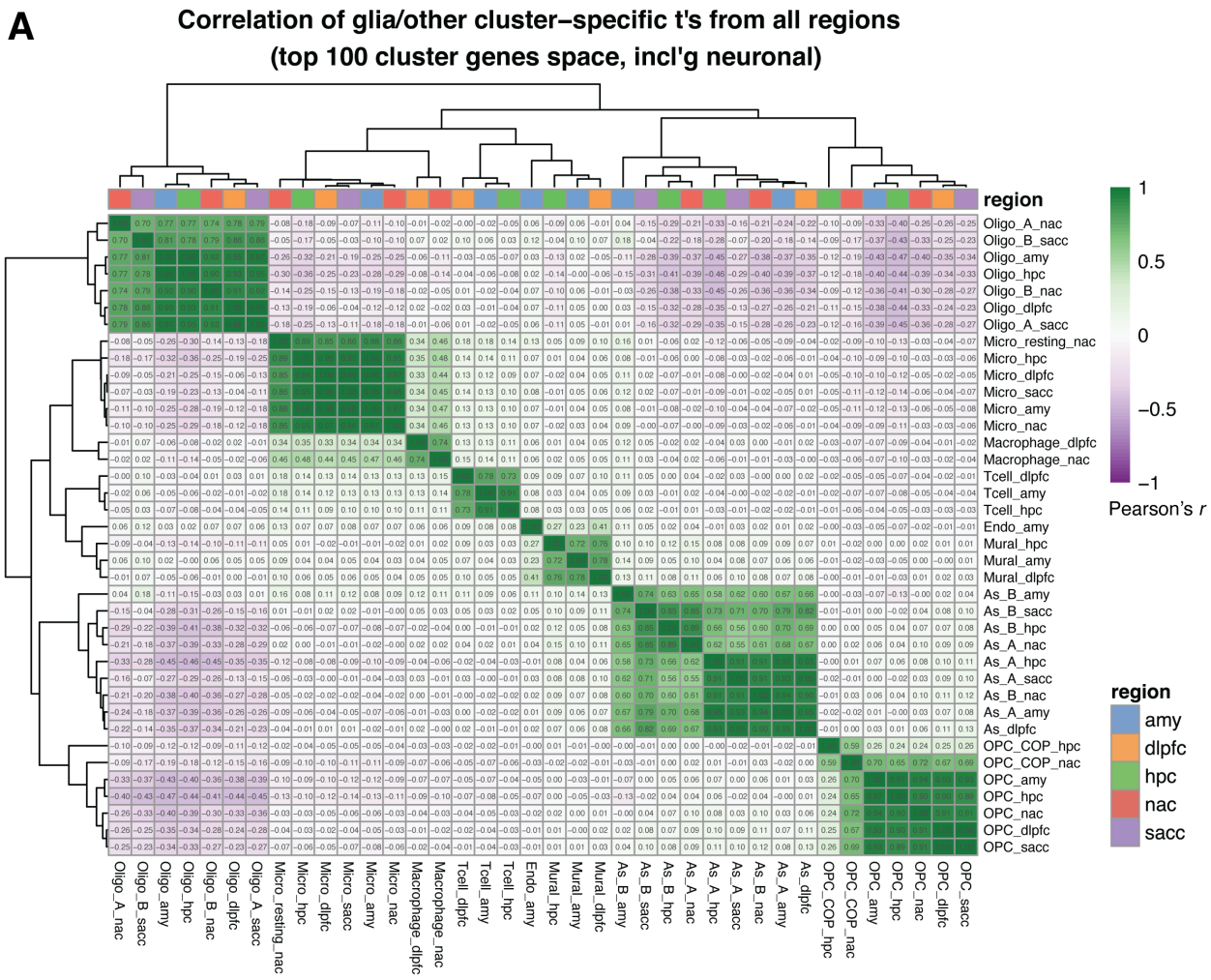

Figure S12. Comparison across all non-neuronal, regionally-defined subpopulations. Pairwise correlation of *t*-statistics, comparing the top cell class marker genes of the total of 107 classes reported across the five brain regions (total of 3,715 genes). Here, only the 38 non-neuronal (glial, stromal, or immune) classes are shown (see **Figure 3B**; **Figure S11**). Regions are colored and labeled in the suffix. Scale values are of Pearson correlation coefficient (*r*).

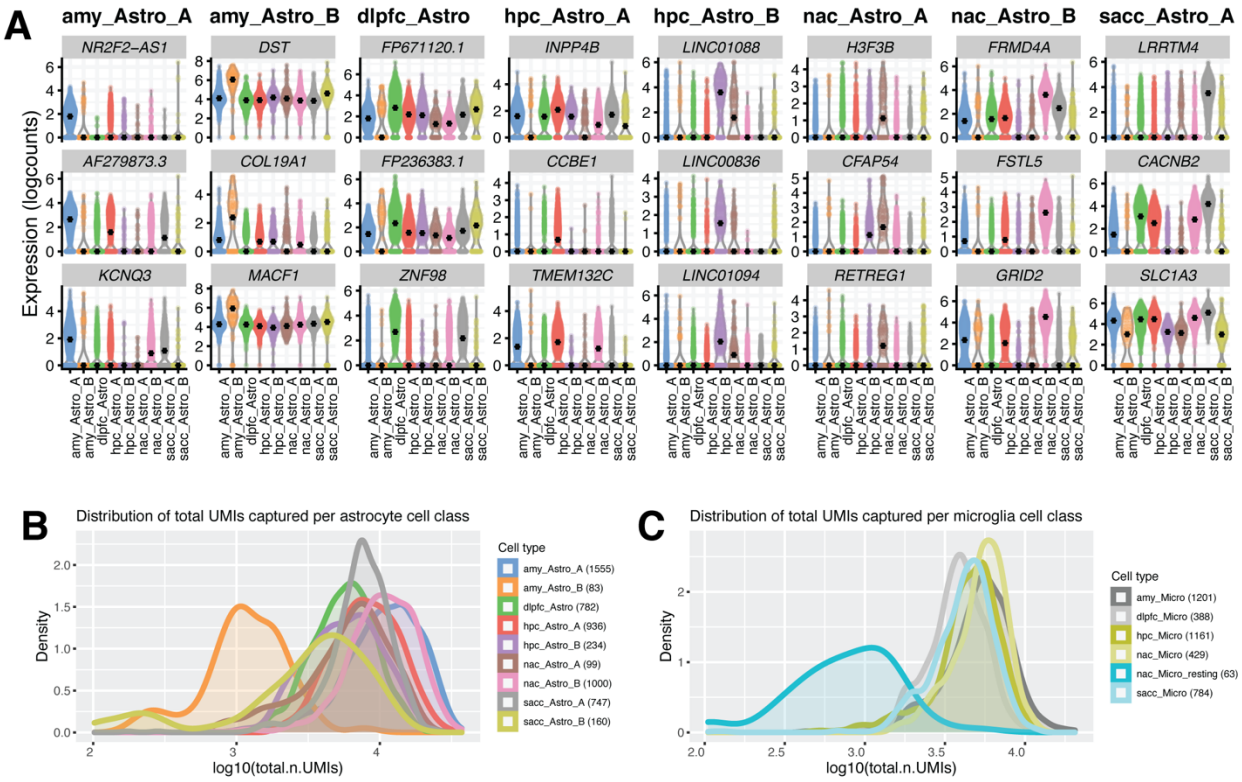

Figure S13. **Across-regions astrocyte differential expression analysis and astrocyte/microglia QC. (A)** Violin plots (scale normalized, log2-transformed, 'logcounts') of the top 3 pairwise-defined markers per regionally-defined astrocyte class. The 'Astro_B' from the sACC had no statistically significant pairwise test-defined markers, so doesn't have its own column (but still showing its corresponding expression in the presented 24 marker genes). **(B)** Density plots for total number of UMIs captured per astrocyte cell class (including sACC 'Astro_B'). Here, we see the AMY 'Astro_B' shows a 10-fold magnitude lower in transcriptional activity than the rest of the astrocytes. **(C)** Similarly, for resting or dormant microglia in the NAc, or 'Micro_resting', its distribution of total number of UMIs captured is an order of magnitude lower than the rest of the defined microglia classes. Related to **Figure 3** and **Figure S12**.

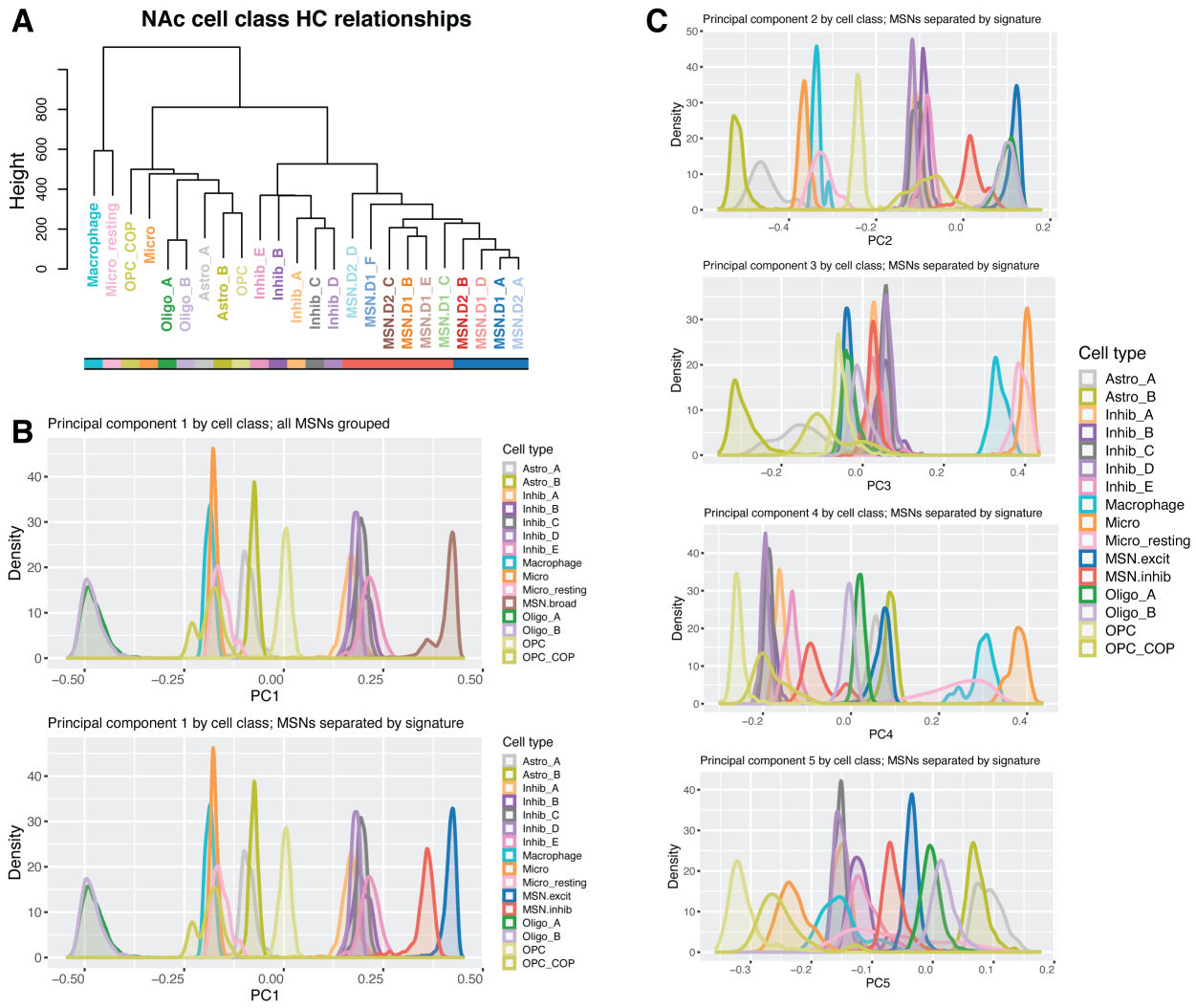

Figure S14. Divergence of MSN class groups by excitatory/inhibitory signature. (A) Hierarchical clustering dendrogram characterizing the relationship between pseudo-bulked profiles of the 24 reported NAc cell classes in **Figure 1** (see Methods). The color bar below the labels shows separation into those D1/D2 MSNs with excitatory transcriptomic signatures (blue, 'MSN.excit': MSN.D1_A/_D and MSN.D2_A/_B) or more inhibitory (red, 'MSN.inhib': MSN.D1_B/_C/_E/_F and MSN.D2_C/_D) when compared to all other neuronal cell classe from the five regions, as per **Figure 3B**. **(B)** Principal component (PC) 1, describing the largest component of variance across all NAc nuclei (see Methods), which separates NAc neuronal classes from glial cell types. MSNs further separate as per these groupings. Above: all MSNs combined (brown); below: binned via their corresponding color bars from the (A). **(C)** PCs 2 through 5, conveying further separation of MSNs by their 'MSN.excit' and 'MSN.inhib' signatures.

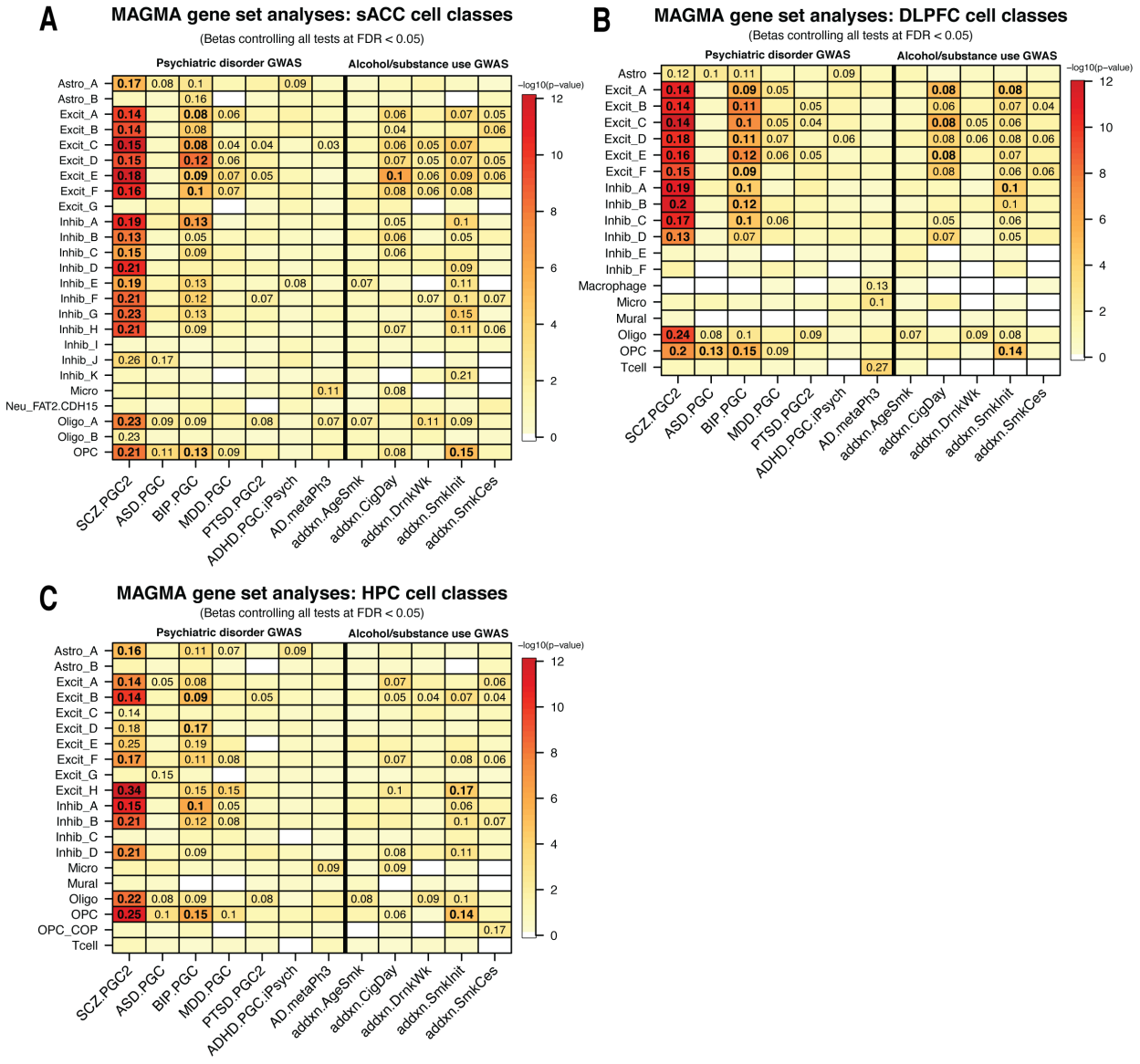

Figure S15. Genetic associations for HPC and cortical regions with psychiatric disease and addiction phenotypes. (A) MAGMA associations for each of 25 cell classes profiled in sACC, **(B)** 19 DLPFC cell classes, and **(C)** 20 HPC cell classes. Related to **Figure 4**; see below for abbreviations. Heatmap is colored by empirical -log10(*p-value*) for each association test. Displayed numbers are the effect size (***β***) for significant associations (controlled for false discovery rate, FDR < 0.05), on a *Z* (standard normal) distribution. Bolded numbers are those that additionally satisfy a strict Bonferroni correction threshold of $p < 3.89e\text{-}5$.
Abbreviations: SCZ: schizophrenia, ASD: autism spectrum disorder, BIP: bipolar disorder, MDD: major depressive disorder, PTSD: posttraumatic stress disorder, ADHD: attention deficit/hyperactivity disorder, AD: Alzheimer's disease. The suffix for these (e.g. '.PGC2') reference the specific study (see Methods). For the (Liu et al., 2019) phenotypes, 'addxn.': "addiction"; 'AgeSmk': age of initiation of regular smoking, 'CigDay': number of cigarettes per day, 'DrnkWk': number of drinks per week, 'SmkInit': whether regular smoking was ever reported, 'SmkCes': if so, had an individual stopped smoking

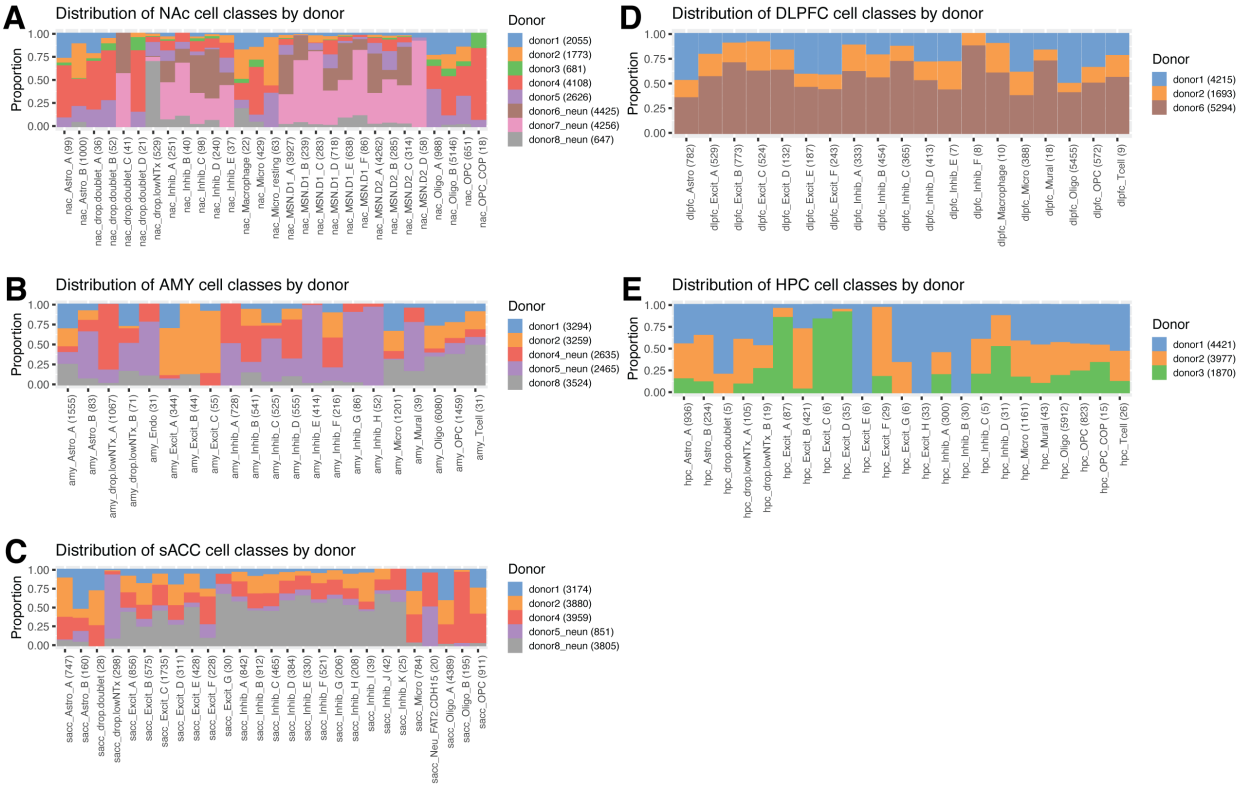

Figure S16. Distribution of regionally-defined cell classes by donor. Distribution of all 107 regionally-defined cell classes and their proportions by donor for **(A)** NAc, **(B)** AMY, **(C)** sACC, **(D)** DLPFC, and **(E)** HPC. Included are each region's technical artifact-driven clusters (total of 12), which are annotated with the 'drop.' prefix and: 'doublet', if they were flagged for high median 'doubletScore' (see Methods), in addition to expressing multiple broad cell class markers (not shown); or 'lowNTx' (for "low number of transcripts"): clusters driven by low quality nuclei or those that captured ambient transcripts/UMIs, yet passed nuclei calling. Related to STAR Methods and **Table S3**.